Published in final edited form as:
Neuroimage. 2011 July 1; 57(1): 242–250. doi:10.1016/j.neuroimage.2011.04.023.

Preparatory Activity and Connectivity in Dorsal Anterior Cingulate Cortex for Cognitive Control

Kurt P. Schulz[a,*], **Anne-Claude V. Bédard**[a], **Rosa Czarnecki**[c], and **Jin Fan**[a,b,c]

[a]Department of Psychiatry, The Mount Sinai School of Medicine, New York, NY, USA

[b]Department of Neuroscience, The Mount Sinai School of Medicine, New York, NY, USA

[c]Department of Psychology, Queens College, The City University of New York, New York, NY, USA

Abstract

Dorsal anterior cingulate cortex (dACC) is composed of functionally distinct subregions that may contribute to the top-down control of response selection and preparation. Multiple motor areas have been identified in dACC, including an anterior zone implicated in conflict monitoring and a caudal zone involved in movement execution. This study tested the involvement of a third cingulate area, the posterior zone of dACC, in the top-down control of response selection and preparation. Sixteen healthy young adults were scanned with event-related functional magnetic resonance imaging while performing a cued go/no-go task that was designed to minimize response conflicts. The activation and functional connectivity of dACC were tested with standard convolution models and psychophysiological interaction analyses, respectively. Ready cues that informed the direction of the impending response triggered preparatory neural activity in the posterior zone of dACC and strengthened functional connectivity with the anterior and caudal zones of dACC, as well as perigenual anterior cingulate cortex, frontal operculum, dorsolateral prefrontal cortex, sensory association cortices, and extra-pyramidal motor areas. The preparatory cues activated dACC above and beyond the general arousing effects common to cues despite negligible conflict in the go/no-go task. The integration of cognitive, sensorimotor, and incentive signals in dACC places the region in an ideal position to select and prepare appropriate behavioral responses to achieve higher-level goals.

Introduction

Dorsal anterior cingulate cortex (dACC) has long been implicated in the brain mechanisms that coordinate and integrate the myriad sensorimotor inputs and outputs with neural representations of internal drives and goals to guide behavior in the multitude of contexts encountered in daily life (e.g., Pardo et al., 1990; Posner and Petersen, 1990). These cognitive control processes comprise a broad set of mental operations, including performance or response monitoring, selection of context-appropriate responses, and inhibition of prepotent but context-irrelevant responses, which have ramifications for

*Corresponding author. Department of Psychiatry, Box 1230, The Mount Sinai School of Medicine, One Gustave L. Levy Place, New York, NY 10029, USA. Fax: +1 212 849 2690 kurt.schulz@mssm.edu.

The authors reported no biomedical financial interests or potential conflicts of interest.

multiple cognitive domains (Miyake et al., 2000; Allain et al., 2009; Verwoerd et al., 2009), decision-making (Moore et al., 2008), and daily functions like driving motor vehicles (Fischer et al., 2007). Consequently, increases in dACC activation have been reported on a variety of cognitive tasks, ranging from the Stroop, Simon, and other conflict tasks to go/no-go tests of response inhibition (Buchsbaum et al., 2005; Laird et al., 2005; Nee et al., 2007; Simmonds et al., 2008).

Meta-analytic reviews have consistently found activation of dACC on go/no-go tests (Buchsbaum et al., 2005; Nee et al., 2007; Simmonds et al., 2008). Yet, there is consensus in the literature that this dACC activation is not specifically related to the inhibition of prepotent responses on the task (Garavan et al., 1999; Braver et al., 2001; Liddle et al., 2001). Instead, dACC activation on go/no-go tasks has been attributed to the occurrence of competing response options, specifically between the prepotent response tendency and the need to inhibit this tendency (Braver et al., 2001; Botvinick et al., 2004; Carter and van Veen, 2007; Banich, 2009). However, conflict cannot fully account for dACC activity during go/no-go tests (Simmonds et al., 2008), the simplest of which involve minimal competition between response options (Picard and Strick, 2001). Rather, dACC activation on no-go trials has been ascribed to such basic response-related processes as the selection of context-appropriate no-go responses (‘no button press’) (Picard and Strick, 2001) or alternatively, selecting to withhold (inhibit) context-inappropriate go responses (‘button press’) (Mostofsky and Simmonds, 2008). Further, differential dACC responses to the presence or absence of conflict on the same task point to the existence of distinct functional regions (Milham et al., 2002; Milham and Banich, 2005).

Convergent lines of evidence support the functional differentiation of dACC into distinct subdivisions that subserve conflict-related and more basic response-related processes (Picard and Strick, 2001). Dorsal ACC contains three distinct motor areas, including a caudal cingulate zone (CCZ) located adjacent to the primary motor cortex that has been linked to movement execution and a rostral cingulate zone that can be subdivided into anterior and posterior divisions (Picard and Strick, 2001; Fan et al., 2008). The anterior rostral cingulate zone (RCZa), which lies medial to and is interconnected with dorsolateral prefrontal cortex (DLPFC) (Barbas and Pandya, 1989), is the site of most conflict-specific dACC activation (Laird et al., 2005; Nee et al., 2007). In contrast, response-related activation has been reported in the posterior rostral cingulate zone (RCZp) regardless of the presence or absence of conflict (Milham and Banich, 2005; Brown, 2009) and even in anticipation of the actual response (Fan et al., 2007; Aarts et al., 2008; Clerkin et al., 2009). The RCZp is ideally positioned to exert top-down control over response processes through extensive reciprocal connections with adjacent premotor and supplementary motor areas (Bates and Goldman-Rakic, 1993), as well as through direct cingulospinal and cingulostriatal tracts (Dum and Strick, 1991; Kunishio and Haber, 1994). Thus, no-go activation of dACC likely reflects the top-down control that RCZp exerts over pre-response or preparatory processes that precede response inhibition.

The nature of go/no-go tasks has complicated the effort to more precisely define the cognitive control functions of dACC. The rapid, continuous presentation of go and no-go targets entails that distinct preparatory and response-related processes occur virtually simultaneously and cannot be separated using standard neuroimaging techniques. We therefore designed a cued go/no-go paradigm that temporally segregated preparatory motor programming and the selection to execute or inhibit responses. Ready cues informed the direction of the impending response (left or right) and after a brief interval go and no-go targets signaled whether to execute or inhibit the prepared response. The task used simple, invariant stimulus-response associations for cues and targets to minimize response conflicts. Event-related functional magnetic resonance imaging (fMRI) was conducted to test the

involvement of dACC in the top-down control of response selection and preparation in healthy adults. Standard convolution models and psychophysiological interaction (PPI) analyses were conducted to test both the activation and functional connectivity of dACC during response preparation. It was hypothesized that ready cues that informed the direction of the impending response would recruit the RCZp to exert top-down control over pre-response or preparatory processes, which would enhance the functional connections with afferent and efferent regions in DLPFC, premotor and supplementary motor areas, and striatum.

Methods

Participants

Participants were 16 healthy, right-handed adults (8 males, mean age = 23.6 ± 4.1 years, range = 18 – 35 years) with normal or corrected-to-normal vision. All participants were screened for psychiatric, neurological, or systemic medical illness and completed the Conners Adult ADHD Rating Scale-Self-Report: Long Version (CAARS) (Conners, 1997) and the Symptom Checklist – 90 – Revised (SCL-90-R) (Derogatis, 1977). A T-score of one standard deviation above age and/or gender means (i.e., > 60) on the SCL-90-R Global Severity Index or the CAARS Total ADHD Symptoms index was used to screen for clinically significant psychiatric and attention problems that might impact task performance. The mean ± SEM T-score was 56.5 ± 2.7 for the SCL-90-R Global Severity Index and 47.4 ± 2.7 for the CAARS Total ADHD Symptoms. The sample was 43.8% Caucasian, 31.3% Asian, 18.8% Hispanic, and 12.5% African-American. All participants provided written informed consent for participation. The study was approved by the Institutional Review Board of The Mount Sinai School of Medicine.

Cued Go/No-Go Paradigm

The cued go/no-go task was designed as an event-related paradigm that was compiled and run using E-Prime software (Psychology Software Tools, Inc., Pittsburgh, PA). The cues and targets used in the cued go/no-go task are illustrated in Fig. 1. There were two cue conditions: relax cue and ready cue, with the ready condition divided into right and left cues. Ready cues were always followed by targets, with the target condition subdivided into go and no-go signals. No targets followed relax cues. Relax cues were depicted by straight lines, ready cues were denoted by right- and left-pointing arrows, and go and no-go signals were depicted by green and red circles, respectively. These simple, over-learned stimulus-response associations (e.g., right-pointing arrow for “right”, green for “go”) were invariant across the task to prevent the introduction of motor conflicts. There were four trial types that were presented in equal ratios: (1) relax cue, no target; (2) ready cue (left or right), no-go target; (3) ready cue (left), go target; and (4) ready cue (right), go target. This trial configuration ensured that there was a 2:1 ratio of go:no-go targets across the task to enhance the tendency to respond. The trial combinations were pseudorandomized across the 4 runs of 32 trials so that each trial type had an equal probability of preceding and following every other type. The four 252 s runs each began and ended with 30 s of fixation. Each trial started with a cue presented above and below fixation for 250 ms, followed by a fixed 2250 ms interval, after which the target was presented at fixation for 250 ms. A fixed cue-target interval was used to maximize the coherence of the cues and targets. The inter-trial interval was jittered from 3000 – 3500 ms (mean per block = 3250 ms). The average trial duration was 6 s.

Participants were instructed to get ready to respond in the direction of the arrow cue and to press the appropriate button as rapidly as possible for the green circles and to withhold responses for the red circles. Participants responded with the right and left index fingers

using the BrainLogics fiber optic button system (Psychology Software Tools, Inc., Pittsburgh, PA). Responses were recorded on a desktop computer and provided measures of reaction time and accuracy.

Image Acquisition

All participants were scanned on the same 3.0 Tesla Siemens Allegra (Siemens, Erlangen, Germany) head-dedicated MRI scanner. Functional T2*-weighted images depicting the blood oxygenation level-dependent (BOLD) signal were obtained in 4 runs of 101 volumes each using gradient-echo echo-planar images (TR = 2500 ms, TE = 27 ms, flip angle = 82°, FOV = 240 mm, matrix = 64 × 64, slice thickness = 4 mm contiguous, in-plane resolution = 3.75 mm^2). A high-resolution T2-weighted anatomical image was acquired at the same 40 slice locations with a turbo spin-echo (TSE) pulse sequence (TR = 4050 msec, TE = 99 msec, flip angle = 170°, FOV = 240 mm, matrix = 512 × 336, 40 slices, slice thickness = 4 mm contiguous, in-plane resolution = 0.47 mm^2). All images were acquired in the axial plane with slices positioned parallel to the anterior commissure – posterior commissure line.

Standard convolution model for fMRI analysis

Event-related analyses of the functional imaging data were conducted using SPM8 software (Wellcome Department of Imaging Neuroscience, London, UK). The four functional time series for each participant were corrected for slice time acquisition, realigned to the first volume in each series to correct for motion, co-registered to the T2 image, normalized to a standard template (Montreal Neurological Institute), and spatially smoothed with an 8 × 8 × 8 mm full-width at half-maximum (FWHM) Gaussian kernel.

First level analyses were conducted individually for each participant with a general linear model (GLM) to determine the relationship between the observed event-related BOLD signals and regressors that represented expected neural responses to trial events. Regressors were created by convolving a train of delta functions that represented the individual trial events with the default SPM basis function, which consisted of a synthetic hemodynamic response function, composed of two gamma functions (Friston et al., 1998). Five orthogonal regressors were included in a multiple regression model by convolving basis function with delta functions for: (1) all cues, representing the variance shared by ready and relax cues, including visual stimulation, arousal, etc.; (2) ready cues, reflecting variance unique to the preparation of responses; (3) all targets, representing the variance shared by go and no-go targets, including visual stimulation, motor activation, etc.; (4) no-go targets, denoting variance unique to the inhibition of responses; and (5) errors, including no-go targets for false alarms and go targets for misses or incorrect responses. The first and third regressors were supersets that included all conditions in the second regressor and the fourth and fifth regressors, respectively. The six parameters created during motion correction were entered as covariates of no interest in the GLM (Johnstone et al., 2006). Low frequency drifting was filtered with a cut-off period of 128 s and serial correlations were corrected using a first-order autoregressive model.

The specific brain responses were tested by applying appropriate linear contrasts to the parameter estimates for each regressor versus baseline, resulting in four contrast maps (excluding the error contrast) for each participant. The four contrast maps for all participants were entered into second-level random-effects group analyses. The resultant voxel-wise statistical maps were thresholded for significance using a cluster-size algorithm that protects against false-positive results (Hayasaka et al., 2004). The height (intensity) threshold of each voxel was set at $p < 0.001$ and the extent (cluster) threshold was fixed at $p < 0.01$. A Monte Carlo simulation that took into account the image resolution parameters and the 8 mm FWHM smoothing parameter established that a cluster extent of 100 contiguous resampled

voxels ($2 \times 2 \times 2$ mm^3) was necessary to correct for multiple voxel comparisons at $p < 0.001$. The simulation method is described in Slotnick and Schacter (2004).

Psychophysiological interaction (PPI) analysis

Volumes of interest (VOI) were extracted from the peaks of maximal activation in right dACC for the response preparation contrast (x = 16, y = 8, z= 38). Specifically, the seed dACC VOI was defined as a 6-mm radius sphere at the local peak nearest to the relevant coordinates individually for each participant. The mean coordinates of the center of the dACC VOI were x = 14.5 ± 3.8 mm, y = 8.4 ± 1.7 mm, and z = 36.5 ± 2.8 mm. The time series of the first eigenvariate of the dACC VOI BOLD signal, adjusted for the effects of interest, was calculated from the time-series of voxels passing significance in the response preparation contrast within this region. Mean volume of the dACC VOI was 704 ± 238 mm^3.

Psychophysiological interaction (PPI) is a regression-based method of functional connectivity that tests for differences in the regression slope of activation between brain regions due to the differential response to the signal from one region (seed) under the influence of different experimental contexts (Friston et al., 1997; Gitelman et al., 2003). The method computes whole-brain connectivity between the time series of the seed VOI and the time series of all other voxels. Separate PPI analyses were conducted for each participant to determine the functional interactions of the dACC VOI during response preparation.

The time-series data of the first eigenvariate of the seed VOI were temporally filtered and mean corrected as in conventional SPM analysis. Bayesian estimation was used to deconvolve the time series of the BOLD signal to generate the time series of the neuronal signal for the VOI. The time series of the neuronal signal for response preparation was then created, generating a PPI regressor that represented the interaction between the psychological and physiological factors, as well as separate regressors representing the main effect of the response preparation contrast (P regressor) and the baseline dACC time course (Y regressor). These regressors were forward-convolved with the hemodynamic response function, and then entered into a regression model along with effects of no interest, including the six motion correction parameters and sessions.

The resultant images of contrast estimates for each participant were entered into a random effect group analysis that tested for significant differential connectivity to the dACC VOI due to the context manipulations. The significance level for each voxel was set at 0.001, with an extent (cluster) threshold of $p < 0.01$, which was determined as described above.

Post-hoc analysis of directionality in response preparation

Post-hoc analyses were conducted to test for differences in preparatory activity for right and left ready cues (i.e., preparation of right and left button presses). Separate regressors were created for right and left ready cues, as well as for go and no-go targets preceded by right and left ready cues, which along with regressors for all cues and errors were entered into a multiple regression model. Specific brain responses were tested by separately contrasting right and left ready cues versus baseline, resulting in two contrast maps for each participant, which were entered into separate group analyses. The height and extent thresholds were both set at $p < 0.01$ for these exploratory analyses due to the lower power to detect effects. VOI were extracted from peaks of activation identified in dACC and PPI was analyzed using the procedures described above.

Results

Behavioral results

Performance measures on the go/no-go task are presented in Table 1. Task performance was near-perfect. Responses on go trials were faster with the left hand than right hand (t_{15} = 7.98, $p < 0.001$). Participants also made more impulsive errors of commission on no-go trials with the left than right hand ($t_{15} = 2.15$, $p < 0.05$). There were no hand differences for accuracy and omission errors (both $p > 0.10$).

Imaging results

General cue effects—The ready and relax cues had a general activating effect on a distributed fronto-temporoparietal network that is shown in the top panel of Fig. 2 and detailed in Table 2. This network included right frontal operculum, left ventral premotor cortex, and bilateral inferior parietal lobule, which extended dorsally and superiorly to superior parietal lobule in both hemispheres. In addition, cues produced robust BOLD signal increases in right middle temporal gyrus and left fusiform gyrus.

Response preparation—The response preparation contrast revealed BOLD signal increases unique to ready cues in several regions depicted in the bottom panel of Fig. 2 and listed in Table 2. Specifically, preparatory activity was seen in the RCZp of right dACC, with the peak centered at y-coordinate = 9 mm and the cluster extending dorsally to the vertical plane passing through the anterior commissure (VCA). Preparatory activity was also found in left anterior insular cortex, as well as bilaterally in visual association areas in middle occipital gyrus, cerebellar vermis, and in the brainstem, at the level of the red nucleus.

PPI analyses revealed that response preparation also produced significant changes in the functional interaction between the RCZp VOI and several known afferent and efferent brain regions shown in Fig. 3 and Table 3. The RCZp VOI showed increased preparation-dependent interactions intrinsically with several anterior cingulate regions, including the RCZa, proximal and contralateral RCZp, and CCZ. Preparatory cues also enhanced extrinsic RCZp connectivity with right frontal operculum and left DLPFC, as well as with bilateral caudate nucleus, left cerebellum, and sensory association cortex in right middle temporal gyrus. In contrast, response preparation increased the negative correlation between activity in the RCZp VOI and right posterior cingulate cortex (PCC), left ventral premotor cortex, bilateral pre-supplementary motor area, bilateral lingual gyrus, and bilateral thalamus.

Post-hoc analyses identified differences in preparatory activity and functional connectivity elicited by right and left ready cues in dACC. As shown in Fig. 4, ready cues elicited dACC activation contralateral to the cued side/response, with left cues recruiting right dACC and right cues engaging left dACC. The peaks of both clusters were centered at y-coordinate = 12 mm, within the RCZp area of dACC. Otherwise, right and left ready cues generated similar patterns of preparatory activity in bilateral inferior frontal gyrus, premotor cortex, and fusiform gyrus (Table 4). Further, the two ready cues also elicited differences in functional connectivity between the left and right RCZp clusters and prefrontal (i.e., dorsolateral vs. ventrolateral), sensory association (i.e., inferior parietal vs. inferior temporal), and subcortical areas (i.e., caudate vs. cerebellum) (Table 5).

General response effects—Targets had a general activating effect on a distributed fronto-parieto-subcortical circuit shown in the top panel of Fig. 5 and listed in Table 6. The general effects of targets only partially overlapped with the general effects of cues. Response-related BOLD signal increases were seen in left frontal operculum, right anterior

insula cortex, bilateral primary motor cortex and supplementary motor area (SMA), as well as bilaterally in inferior parietal lobule. This circuit also extended subcortically to cerebellum bilaterally and to left thalamus.

Response inhibition—The response inhibition contrast identified no-go-unique BOLD signal increases in the frequently described frontoparietal network depicted in the bottom panel of Fig. 5 and listed in Table 6. In particular, inhibition-related activation was seen in the pars orbitalis of left inferior frontal gyrus and the pars triangularis of right inferior frontal gyrus, right middle frontal gyrus (MFG) extending rostrally to pre-SMA, and left ventral premotor cortex. No-go targets also had unique effects on attention regions along the temporoparietal cortical junction and on visual association areas in anterior middle temporal gyrus and more dorsally in right middle occipital gyrus.

Discussion

The current results provide evidence that dACC contributes to the top-down control of pre-response or preparatory processes. Ready cues that informed the direction of the impending response triggered preparatory neural activity in the RCZp area of right dACC and strengthened functional connections intrinsically with RCZa and all three motor areas in dACC, as well as extrinsically with DLPFC, frontal operculum, cerebellum, sensory association cortices, and extra-pyramidal motor areas. Further, the preparatory activation varied uniquely in RCZp according to the direction of the response cued, with left cues recruiting right dACC and right cues engaging left dACC. Interestingly, an accuracy-for-speed trade-off for left-handed responses may account for the predominance of right dACC activation. RCZp activation was unique to preparatory cues, above and beyond the general arousing or activating properties common to cues (Hackley and Valle-Inclan, 2003), and was not seen for target-related response execution and inhibition processes that have previously been linked to dACC function (Laird et al., 2005; Nee et al., 2007). The cue-triggered dACC activation is particularly revealing regarding the role of dACC in cognitive control since the go/no-go task involved negligible conflict; each cue and target was associated with a single response option and each response option was associated with a single cue or target. These findings confirm that activation of dACC during cued go/no-go tasks reflects the preparatory selection and motor programming of context-appropriate responses rather than the later selection to execute or inhibit responses.

The absence of any dACC activation associated with response inhibition in the current study is surprising and provides clues about the nature of this cognitive control mechanism. Meta-analyses have consistently reported dACC activation associated with response inhibition on no-go trials of go/no-go tasks (Buchsbaum et al., 2005; Nee et al., 2007; Simmonds et al., 2008), which has been presumed to reflect response selection processes, specifically selecting to not respond on no-go trials (Picard and Strick, 2001; Mostofsky and Simmonds, 2008). However, the current results argue for a slight modification of this view of dACC function during response inhibition. The activation of dACC during the cue-triggered selection of right and left responses rather than during the later selection of responding or not responding to targets implicates dACC in pre-response or preparatory motor programming, regardless of whether the response is made or inhibited. These distinct response selection processes, which transpire on the order of hundreds of milliseconds, and occur virtually simultaneously in response to go and no-go targets during a traditional go/no-go task, will be indexed by the same fMRI-BOLD signal, making the processes indistinguishable in most studies.

The pattern of activation and connectivity in the RCZp area of dACC is consistent with theories that postulate its involvement in response selection (Picard and Strick, 2001) and

the control of volitional action (Paus, 2001). This region of dACC, along with anterior insular cortex that was also activated by preparatory cues and frontal operculum with which it is functionally connected, comprise a network that has been implicated in the cued implementation of task-sets in downstream sensorimotor processors (Dosenbach et al., 2006; 2007). This is reflected in the current study in the cue-triggered functional connectivity between dACC and temporal sensory association cortices, cerebellum, and extra-pyramidal motor areas in caudate nuclei, which correspond to known cingulotemporal (Pandya et al., 1981) and cingulostriatal pathways (Kunishio and Haber, 1994). In particular, functional interactions with frontal operculum provide dACC with access to motor representations of goal-directed hand actions (i.e., button presses) (Iacoboni and Wilson, 2006) and indirect influence on the primary motor cortex (Miyachi et al., 2005). Moreover, the interaction between RCZp and downstream sensorimotor processors depends on the nature of the response being prepared. Thus, RCZp may interact with supplementary motor area during involuntary, non-conscious sensorimotor processes (Boy et al., 2010). Conversely, negative correlations in activity between dACC and afferent regions in pre-supplementary motor area, premotor cortex, and primary visual cortex may reflect the inhibition of potentially intrusive sensorimotor input during the preparatory period. These functional interactions may underlie the effects of the contingent negative variation event-related potential that is generated in dACC and adjacent regions (Nagai et al., 2004; Fan et al., 2007), which primes task-relevant cortical regions to process targets more efficiently (Gomez et al., 2004).

Functional interactions between dACC and DLPFC are a central component of most cognitive control models (Carter et al., 1998; Paus, 2001; Botvinick et al., 2004; Carter and van Veen, 2007; Banich, 2009). The strengthened connectivity between RCZp and DLPFC during response preparation in the current study is consistent with a previous meta-analysis that found a greater-than-chance frequency of concomitant activation of the two regions across multiple tasks (Koski and Paus, 2000). The current finding is also comparable to a previous report of increased dACC – DLPFC connectivity during conflict processing (Fan et al., 2008). The conflict-dependent interactions may signal either DLPFC to increase top-down control (Kerns et al., 2004) or dACC to resolve response-related conflicts (Silton et al., 2010). However, the separate brain networks that mediate response anticipation and conflict processing have been found to overlap at the cusp of the anterior and posterior rostral cingulate zones of dACC (Fan et al., 2007). Thus, the strengthening of dACC – DLPFC connectivity might facilitate response selection and preparation in a manner similar to that reported for conflict processing, by increasing the top-down control of response processes (Kerns et al., 2004; Fan et al., 2008; Fan et al., in press) or facilitating response selection and task-set implementation (Silton et al., 2010). These data clearly demonstrate that top-control cognitive control is engaged during response selection and preparation. However, this engagement may be transient and taskdependent since an influential meta-analysis found no functional connectivity between dACC and DLPFC during the resting state (Dosenbach et al., 2007).

The cue-triggered functional connectivity between the various subdivisions of dACC in the current study is partially consistent with a previous report of dACC functional integration during conflict processing (Fan et al., 2008). Response conflict was found to increase the functional connectivity from RCZa to CCZ of dACC. In contrast, response preparation was associated with increased functional interactions between RCZp and both RCZa and CCZ of dACC in the current study. RCZp was also found to have robust preparation-dependent interactions with the perigenual affective division of anterior cingulate cortex (Bush et al., 2000). This perigenual anterior cingulate region receives extensive limbic input (Kunishio and Haber, 1994) and has been implicated in the evaluation of the salience of emotional and motivational information (Vogt et al., 1992). Reports of negative connectivity between dACC and rostral anterior cingulate cortex during the resting state (e.g., Margulies et al.,

2007) suggest that the current findings of preparation-dependent connectivity may provide dACC with transient, taskdependent input on the reinforcing properties of response options. The observed integration of the cognitive and affective divisions of the anterior cingulate cortex may reflect the networks that facilitate response selection and preparation.

The integration of cognitive, sensorimotor, and incentive signals in dACC places this region in an ideal position to monitor context and select and prepare appropriate behavioral responses to achieve any number of higher-level goals. In fact, dACC has been proposed to be part of a core "task-mode" network that supports performance during attention-demanding tasks in opposition to a "default-mode" network that is non-goal directed and more metabolically active during the resting state (Greicius et al., 2003; Fox et al., 2005). The anti-correlated activity in these two networks is reflected in the current finding of negatively correlated activity in dACC and PCC, which together with precuneus and medial prefrontal cortex/rostral cingulate cortex comprise the default-mode network (Fox et al., 2005). Reduced activity in dACC and a failure to suppress activity in the default-mode network has been associated with transient lapses in attention (Weissman et al., 2006) and errors on a conflict task (Fan et al., 2008). The low error rate in the current study regrettably precluded testing the association between dACC and default-mode activation and performance on the go/no-go task. Nonetheless, the anticorrelated activity in dACC and PCC further confirms that response preparation engages top-down cognitive control mechanisms in dACC.

These findings must be considered in the context of a methodological limitation imposed by the cued go/no-go task. The cued go/no-go task was designed with a fixed rather than a jittered cue-target interval in order to maximize the coherence of the cues and targets. The jittered interval and partial trials (i.e., cue only) that have traditionally been used to deconvolve the actual hemodynamic response functions for cues and targets changes the cue-target relationship and attenuates the effect of cues on neural activity. We instead used a 2250 ms cue-target interval, which together with the default SPM8 hemodynamic response function, should have been long enough to detect the cue-target differences and to model the corresponding neuronal signals (Buckner, 1998). We have previously used this analytic approach to successfully isolate preparatory and motor signals associated with cues and targets (Clerkin et al., 2009).

In summary, the current results provide evidence that activation of dACC during a cued go/no-go task reflects the preparatory selection and motor programming of context-appropriate responses rather than the later selection to execute or inhibit responses. Ready cues that informed the direction of the impending response on the go/no-go task recruited RCZp to exert top-down control over preparatory processes, which enhanced the functional connections with afferent and efferent regions in DLPFC, premotor and supplementary motor areas, and striatum. Thus, dACC is ideally positioned to monitor context and select and prepare appropriate behavioral responses to achieve any number of higher-level goals.

Acknowledgments

This research was supported by National Institutes of Health Grant K01MH070892 to Kurt Schulz. The authors thank Hannah Oltarzewska for assistance during data collection.

References

Aarts E, Roelofs A, van Turennout M. Anticipatory activity in anterior cingulate cortex can be independent of conflict and error likelihood. J Neurosci. 2008; 28:4671–4678. [PubMed: 18448644]

Allain S, Burle B, Hasbroucq T, Vidal F. Sequential adjustments before and after partial errors. Psychon Bull Rev. 2009; 16:356–362. [PubMed: 19293107]

Banich MT. Executive function: search for an integrated account. Current Directions in Psychological Science. 2009; 18:89–94.

Barbas H, Pandya DN. Architecture and intrinsic connections of the prefrontal cortex in the rhesus monkey. J Comp Neurol. 1989; 286:353–375. [PubMed: 2768563]

Bates JF, Goldman-Rakic PS. Prefrontal connections of medial motor areas in the rhesus monkey. J Comp Neurol. 1993; 336:211–228. [PubMed: 7503997]

Botvinick MM, Cohen JD, Carter CS. Conflict monitoring and anterior cingulate cortex: an update. Trends Cogn Sci. 2004; 8:539–546. [PubMed: 15556023]

Boy F, Husain M, Singh KD, Sumner P. Supplementary motor area activations in unconscious inhibition of voluntary action. Exp Brain Res. 2010; 206:441–448. [PubMed: 20871983]

Braver TS, Barch DM, Gray JR, Molfese DL, Snyder A. Anterior cingulate cortex and response conflict: effects of frequency, inhibition and errors. Cereb Cortex. 2001; 11:825–836. [PubMed: 11532888]

Brown JW. Conflict effects without conflict in anterior cingulate cortex: multiple response effects and context specific representations. Neuroimage. 2009; 47:334–341. [PubMed: 19375509]

Buchsbaum BR, Greer S, Chang WL, Berman KF. Meta-analysis of neuroimaging studies of the Wisconsin card-sorting task and component processes. Hum Brain Mapp. 2005; 25:35–45. [PubMed: 15846821]

Buckner RL. Event-related fMRI and the hemodynamic response. Hum Brain Mapp. 1998; 6:373–377. [PubMed: 9788075]

Bush G, Luu P, Posner MI. Cognitive and emotional influences in anterior cingulate cortex. Trends Cogn Sci. 2000; 4:215–222. [PubMed: 10827444]

Carter CS, Braver TS, Barch DM, Botvinick MM, Noll D, Cohen JD. Anterior cingulate cortex, error detection, and the online monitoring of performance. Science. 1998; 280:747–749. [PubMed: 9563953]

Carter CS, van Veen V. Anterior cingulate cortex and conflict detection: an update of theory and data. Cogn Affect Behav Neurosci. 2007; 7:367–379. [PubMed: 18189010]

Clerkin SM, Schulz KP, Halperin JM, Newcorn JH, Ivanov I, Tang CY, Fan J. Guanfacine potentiates the activation of prefrontal cortex evoked by warning signals. Biological psychiatry. 2009; 66:307–312. [PubMed: 19520360]

Conners, CK. Conners' Rating Scales - Revised, Technical Manual. Toronto: Multi-Health Systems; 1997.

Derogatis, LR. CL-90: Administration, scoring and procedures manual-I for the R(evised) version and other instruments of the psychopathology rating scale series. Baltimore, MD: Clinical Psychometrics Research Unit, Johns Hopkins University School of Medicine; 1977.

Dosenbach NU, Fair DA, Miezin FM, Cohen AL, Wenger KK, Dosenbach RA, Fox MD, Snyder AZ, Vincent JL, Raichle ME, Schlaggar BL, Petersen SE. Distinct brain networks for adaptive and stable task control in humans. Proc Natl Acad Sci U S A. 2007; 104:11073–11078. [PubMed: 17576922]

Dosenbach NU, Visscher KM, Palmer ED, Miezin FM, Wenger KK, Kang HC, Burgund ED, Grimes AL, Schlaggar BL, Petersen SE. A core system for the implementation of task sets. Neuron. 2006; 50:799–812. [PubMed: 16731517]

Dum RP, Strick PL. The origin of corticospinal projections from the premotor areas in the frontal lobe. J Neurosci. 1991; 11:667–689. [PubMed: 1705965]

Fan J, Gu X, Liu X, Guise KG, Park Y, Martin L, de Marchena A, Tang CY, Minzenberg MJ, Hof PR. Involvement of the anterior cingulate and frontoinsular cortices in rapid processing of salient facial emotional information. Neuroimage. in press.

Fan J, Hof PR, Guise KG, Fossella JA, Posner MI. The functional integration of the anterior cingulate cortex during conflict processing. Cereb Cortex. 2008; 18:796–805. [PubMed: 17652463]

Fan J, Kolster R, Ghajar J, Suh M, Knight RT, Sarkar R, McCandliss BD. Response anticipation and response conflict: an event-related potential and functional magnetic resonance imaging study. J Neurosci. 2007; 27:2272–2282. [PubMed: 17329424]

Fischer M, Barkley RA, Smallish L, Fletcher K. Hyperactive children as young adults: driving abilities, safe driving behavior, and adverse driving outcomes. Accident; analysis and prevention. 2007; 39:94–105.

Fox MD, Snyder AZ, Vincent JL, Corbetta M, Van Essen DC, Raichle ME. The human brain is intrinsically organized into dynamic, anticorrelated functional networks. Proc Natl Acad Sci U S A. 2005; 102:9673–9678. [PubMed: 15976020]

Friston KJ, Buechel C, Fink GR, Morris J, Rolls E, Dolan RJ. Psychophysiological and modulatory interactions in neuroimaging. Neuroimage. 1997; 6:218–229. [PubMed: 9344826]

Friston KJ, Fletcher P, Josephs O, Holmes A, Rugg MD, Turner R. Event-related fMRI: characterizing differential responses. Neuroimage. 1998; 7:30–40. [PubMed: 9500830]

Garavan H, Ross TJ, Stein EA. Right hemispheric dominance of inhibitory control: an event-related functional MRI study. Proc Natl Acad Sci U S A. 1999; 96:8301–8306. [PubMed: 10393989]

Gitelman DR, Penny WD, Ashburner J, Friston KJ. Modeling regional and psychophysiologic interactions in fMRI: the importance of hemodynamic deconvolution. Neuroimage. 2003; 19:200–207. [PubMed: 12781739]

Gomez CM, Fernandez A, Maestu F, Amo C, Gonzalez-Rosa JJ, Vaquero E, Ortiz T. Task-specific sensory and motor preparatory activation revealed by contingent magnetic variation. Brain Res Cogn Brain Res. 2004; 21:59–68. [PubMed: 15325413]

Greicius MD, Krasnow B, Reiss AL, Menon V. Functional connectivity in the resting brain: a network analysis of the default mode hypothesis. Proc Natl Acad Sci U S A. 2003; 100:253–258. [PubMed: 12506194]

Hackley SA, Valle-Inclan F. Which stages of processing are speeded by a warning signal? Biol Psychol. 2003; 64:27–45. [PubMed: 14602354]

Hayasaka S, Phan KL, Liberzon I, Worsley KJ, Nichols TE. Nonstationary cluster-size inference with random field and permutation methods. Neuroimage. 2004; 22:676–687. [PubMed: 15193596]

Iacoboni M, Wilson SM. Beyond a single area: motor control and language within a neural architecture encompassing Broca's area. Cortex. 2006; 42:503–506. [PubMed: 16881259]

Johnstone T, Ores Walsh KS, Greischar LL, Alexander AL, Fox AS, Davidson RJ, Oakes TR. Motion correction and the use of motion covariates in multiple-subject fMRI analysis. Hum Brain Mapp. 2006; 27:779–788. [PubMed: 16456818]

Kerns JG, Cohen JD, MacDonald AW 3rd, Cho RY, Stenger VA, Carter CS. Anterior cingulate conflict monitoring and adjustments in control. Science. 2004; 303:1023–1026. [PubMed: 14963333]

Koski L, Paus T. Functional connectivity of the anterior cingulate cortex within the human frontal lobe: a brain-mapping meta-analysis. Exp Brain Res. 2000; 133:55–65. [PubMed: 10933210]

Kunishio K, Haber SN. Primate cingulostriatal projection: limbic striatal versus sensorimotor striatal input. J Comp Neurol. 1994; 350:337–356. [PubMed: 7533796]

Laird AR, McMillan KM, Lancaster JL, Kochunov P, Turkeltaub PE, Pardo JV, Fox PT. A comparison of label-based review and ALE meta-analysis in the Stroop task. Hum Brain Mapp. 2005; 25:6–21. [PubMed: 15846823]

Liddle PF, Kiehl KA, Smith AM. Event-related fMRI study of response inhibition. Hum Brain Mapp. 2001; 12:100–109. [PubMed: 11169874]

Margulies DS, Kelly AM, Uddin LQ, Biswal BB, Castellanos FX, Milham MP. Mapping the functional connectivity of anterior cingulate cortex. Neuroimage. 2007; 37:579–588. [PubMed: 17604651]

Milham MP, Banich MT. Anterior cingulate cortex: an fMRI analysis of conflict specificity and functional differentiation. Hum Brain Mapp. 2005; 25:328–335. [PubMed: 15834861]

Milham MP, Erickson KI, Banich MT, Kramer AF, Webb A, Wszalek T, Cohen NJ. Attentional control in the aging brain: insights from an fMRI study of the stroop task. Brain Cogn. 2002; 49:277–296. [PubMed: 12139955]

Miyachi S, Lu X, Inoue S, Iwasaki T, Koike S, Nambu A, Takada M. Organization of multisynaptic inputs from prefrontal cortex to primary motor cortex as revealed by retrograde transneuronal transport of rabies virus. J Neurosci. 2005; 25:2547–2556. [PubMed: 15758164]

Miyake A, Friedman NP, Emerson MJ, Witzki AH, Howerter A, Wager TD. The unity and diversity of executive functions and their contributions to complex "Frontal Lobe" tasks: a latent variable analysis. Cogn Psychol. 2000; 41:49–100. [PubMed: 10945922]

Moore AB, Clark BA, Kane MJ. Who shalt not kill? Individual differences in working memory capacity, executive control, and moral judgment. Psychol Sci. 2008; 19:549–557. [PubMed: 18578844]

Mostofsky SH, Simmonds DJ. Response inhibition and response selection: two sides of the same coin. J Cogn Neurosci. 2008; 20:751–761. [PubMed: 18201122]

Nagai Y, Critchley HD, Featherstone E, Fenwick PB, Trimble MR, Dolan RJ. Brain activity relating to the contingent negative variation: an fMRI investigation. Neuroimage. 2004; 21:1232–1241. [PubMed: 15050551]

Nee DE, Wager TD, Jonides J. Interference resolution: insights from a meta-analysis of neuroimaging tasks. Cogn Affect Behav Neurosci. 2007; 7:1–17. [PubMed: 17598730]

Pandya DN, Van Hoesen GW, Mesulam MM. Efferent connections of the cingulate gyrus in the rhesus monkey. Exp Brain Res. 1981; 42:319–330. [PubMed: 6165607]

Pardo JV, Pardo PJ, Janer KW, Raichle ME. The anterior cingulate cortex mediates processing selection in the Stroop attentional conflict paradigm. Proc Natl Acad Sci U S A. 1990; 87:256–259. [PubMed: 2296583]

Paus T. Primate anterior cingulate cortex: where motor control, drive and cognition interface. Nat Rev Neurosci. 2001; 2:417–424. [PubMed: 11389475]

Picard N, Strick PL. Imaging the premotor areas. Curr Opin Neurobiol. 2001; 11:663–672. [PubMed: 11741015]

Posner MI, Petersen SE. The attention system of the human brain. Annu Rev Neurosci. 1990; 13:25–42. [PubMed: 2183676]

Silton RL, Heller W, Towers DN, Engels AS, Spielberg JM, Edgar JC, Sass SM, Stewart JL, Sutton BP, Banich MT, Miller GA. The time course of activity in dorsolateral prefrontal cortex and anterior cingulate cortex during top-down attentional control. Neuroimage. 2010; 50:1292–1302. [PubMed: 20035885]

Simmonds DJ, Pekar JJ, Mostofsky SH. Meta-analysis of Go/No-go tasks demonstrating that fMRI activation associated with response inhibition is taskdependent. Neuropsychologia. 2008; 46:224–232. [PubMed: 17850833]

Slotnick SD, Schacter DL. A sensory signature that distinguishes true from false memories. Nat Neurosci. 2004; 7:664–672. [PubMed: 15156146]

Verwoerd J, Wessel I, de Jong PJ. Individual differences in experiencing intrusive memories: the role of the ability to resist proactive interference. J Behav Ther Exp Psychiatry. 2009; 40:189–201. [PubMed: 18929357]

Vogt BA, Finch DM, Olson CR. Functional heterogeneity in cingulate cortex: the anterior executive and posterior evaluative regions. Cereb Cortex. 1992; 2:435–443. [PubMed: 1477524]

Weissman DH, Roberts KC, Visscher KM, Woldorff MG. The neural bases of momentary lapses in attention. Nat Neurosci. 2006; 9:971–978. [PubMed: 16767087]

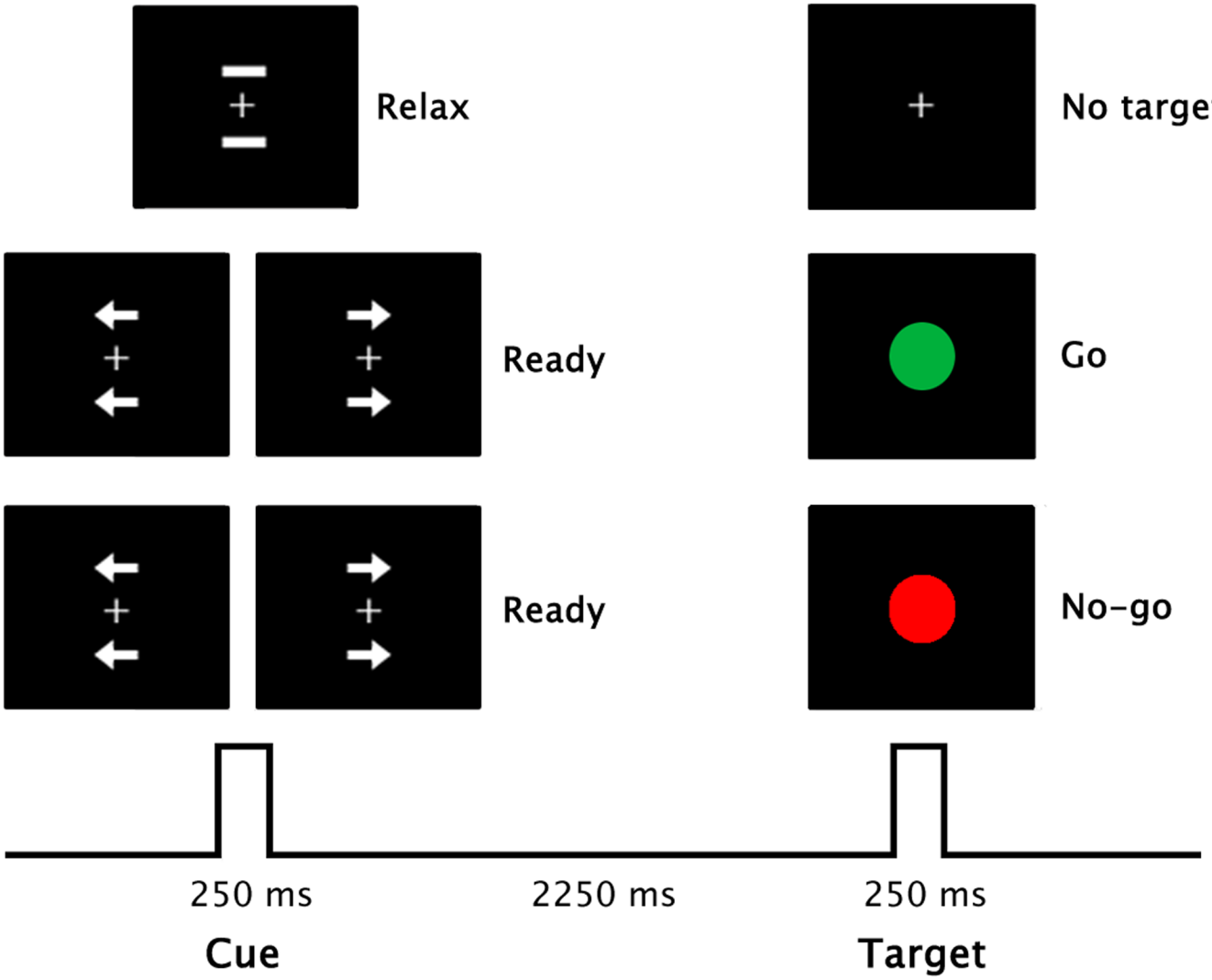

Fig. 1.

Schematic of the cued go/no-go task used to elicit response preparation and response inhibition. Each trial started with a cue presented for 250 ms, followed by a 2250 ms interval, after which the target was presented for 250 ms. The inter-trial interval was jittered from 3000 – 3500 ms. There were two cue conditions: relax cue and ready cue, including right and left cues. There were also two target conditions: no-target and target, including go and no-go targets. The trial configuration ensured a 2:1 ratio of go:no-go targets. Participants had to prepare to respond in the direction of the arrow cue and press the appropriate button as rapidly as possible for the green circles and withhold responses for the red circles.

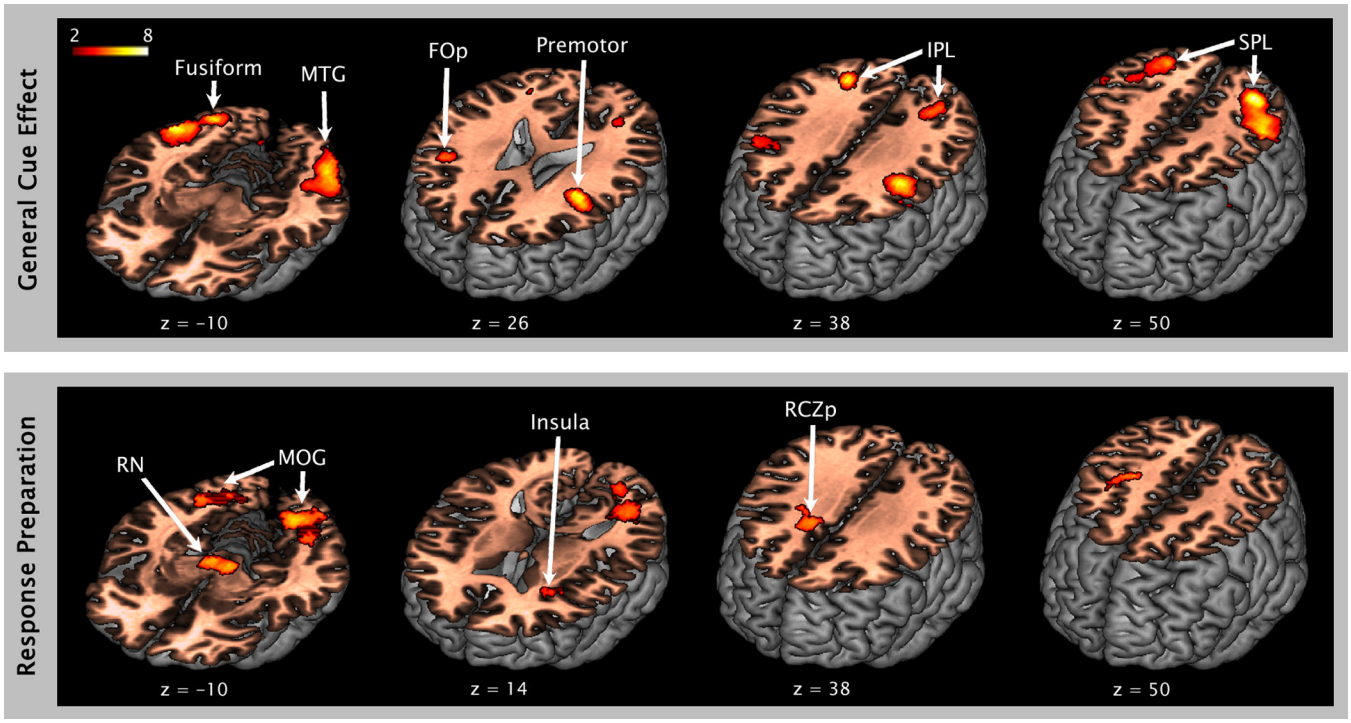

Fig. 2.

Blood oxygen level-dependent (BOLD) signal increases common to all cues (top panel) and specific to response preparation elicited by ready cues (bottom panel). Cues had general activating effects on the frontal operculum (FOp), premotor cortex, inferior parietal lobule (IPL) extending to the superior parietal lobule (SPL), as well as on the fusiform gyrus and middle temporal gyrus (MTG). Ready cues uniquely generated preparatory activity in the posterior rostral cingulate zone (RCZp) of the dorsal anterior cingulate cortex, insula cortex, middle occipital gyrus (MOG), cerebellum, and red nucleus (RN). Values at the bottom of the sections refer to Montreal Neurological Institute coordinates. The color bar represents *t* values. The figures were thresholded at $p < 0.001$, $k = 100$.

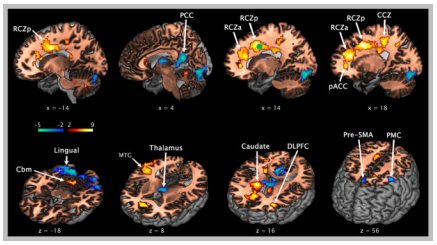

Fig. 3.

Positive and negative psychophysiological interaction (PPI) with the dorsal anterior cingulate cortex during response preparation shown on sagittal (top row) and axial sections (bottom row). The posterior rostral cingulate zone (RCZp) volume of interest (VOI) showed increased preparation-dependent connectivity with the anterior rostral (RCZa), proximal and contralateral RCZp, and caudal cingulate zones (CCZ), as well as the perigenual anterior cingulate cortex (pACC), dorsolateral prefrontal cortex (DLPFC), caudate nucleus, middle temporal gyrus (MTG), and cerebellum (CBM). In contrast, response preparation increased the negative correlations between activity in RCZp and the posterior cingulate cortex (PCC), pre-supplementary motor area (Pre-SMA), ventral premotor cortex (PMC), lingual gyrus, and thalamus. The green dot depicts the mean coordinates of the RCZp VOI as described in the Method section. Values at the bottom of the sections refer to Montreal Neurological Institute coordinates. The color bars represent *t* values. The figures were thresholded at $p < 0.001$, $k = 100$.

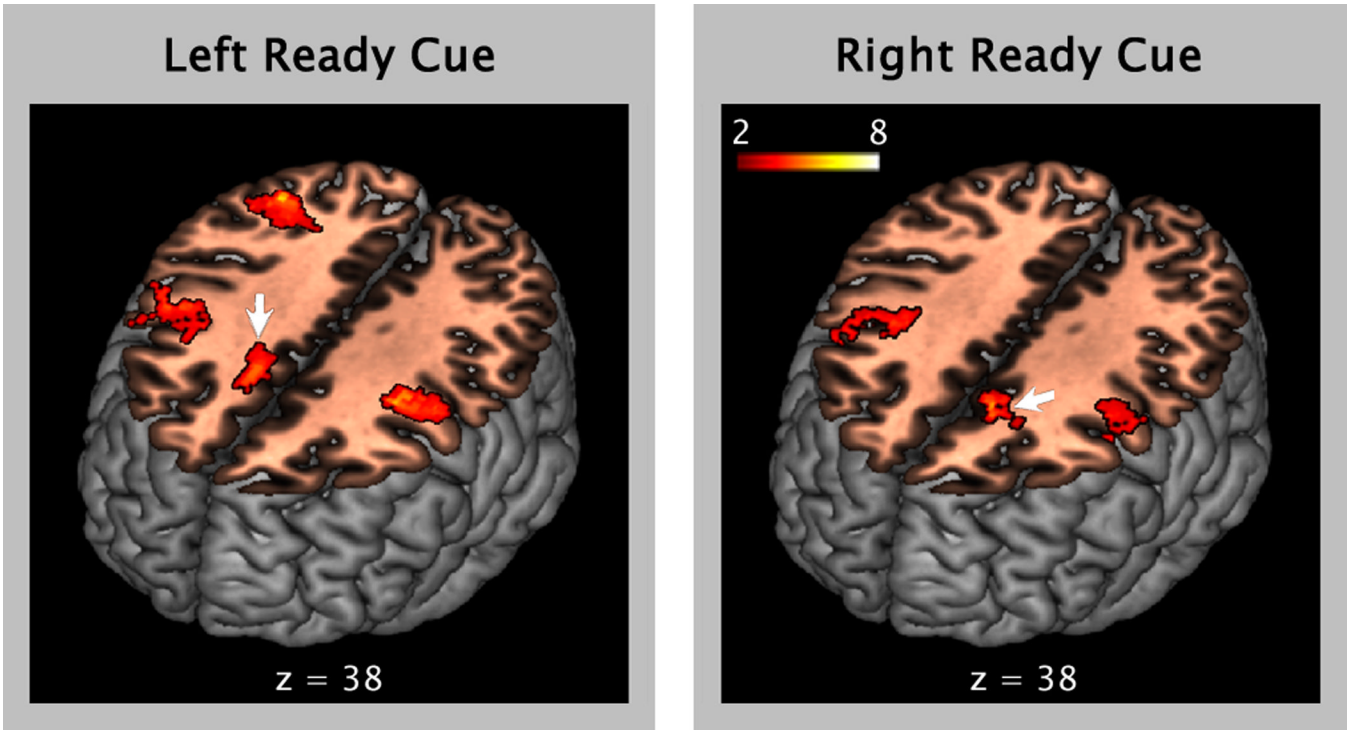

Fig. 4.

Differential blood oxygen level-dependent (BOLD) signal in dorsal anterior cingulate cortex for left and right ready cues. Ready cues elicited dACC activation contralateral to the cued side/response, with the peaks of both clusters centered at y-coordinate = 12 mm, within the RCZp area of dACC. Values at the bottom of the sections refer to Montreal Neurological Institute coordinates. The color bar represents *t* values. The figures were thresholded at $p < 0.01$, $k = 100$.

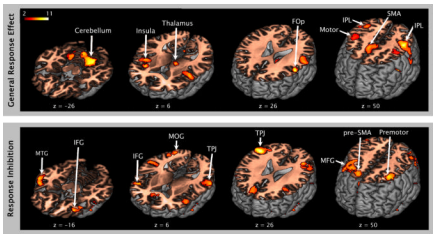

Fig. 5.

Blood oxygen level-dependent (BOLD) signal increases common to go and no-go signals (top panel) and specific to response inhibition elicited by no-go signals (bottom panel). Go and no go signals had general activating effects on the frontal operculum (FOp), anterior insula cortex, primary motor cortex, supplementary motor area (SMA), inferior parietal lobule (IPL), cerebellum, and thalamus. No-go signals produced unique inhibition-related activation in the inferior frontal gyrus (IFG), middle frontal gyrus (MFG) extending to the pre-supplementary motor area (pre-SMA), premotor cortex, temporoparietal cortical junction (TPJ)., middle temporal gyrus (MTG), and middle occipital gyrus (MOG). Values at the bottom of the sections refer to Montreal Neurological Institute coordinates. The color bar represents *t* values. The figures were thresholded at $p < 0.001$, $k = 100$.

Table 1

Mean ± SEM performance on the cued go/no-go task (n = 16).

	Left button	Right button
Go trials		
Correct responses (%)	97.7 ± 1.0	96.3 ± 1.5
Incorrect responses (%)	0.2 ± 0.2	1.7 ± 1.4
Omission errors (%)	2.1 ± 1.0	2.0 ± 0.9
RT (ms) **	414.7 ± 23.4	483.3 ± 27.3
No-go trials		
Commission errors (%) *	3.5 ± 1.4	0.8 ± 0.5

* Note: $p < 0.05$

** $p < 0.001$.

Table 2

BOLD signal increases common to all cues and specific to response preparation elicited by ready cues

Peak	Side	BA	MNI coordinates			Cluster size (κ)	*T*-value
			x	*y*	*z*		
General cue effects							
Frontal operculum	R	44	46	12	28	183	4.77
Ventral premotor cortex	L	6	−40	2	30	564	7.63
Inferior parietal lobule	R	40	36	−62	38	915	7.12
Inferior parietal lobule	L	40	−30	−58	52	1,637	8.16
Middle temporal gyrus	R	21	56	−56	2	1,724	7.80
Fusiform gyrus	L	19	−42	−64	−14	2,016	6.94
Response preparation							
Dorsal anterior cingulate cortex	R	24/32	16	8	38	1,110	4.58
Anterior insula cortex	L	---	−30	26	14	133	3.94
Middle occipital gyrus	R	19	38	−76	−2	4,058	8.20
Middle occipital gyrus	L	19	−34	−76	−2	7,643	6.61
Cerebellum (vermis)	B	---	8	−62	−28	392	4.39
Brainstem (red nucleus)	B	---	6	−22	−12	583	5.27

Note: BA = Brodmann area; B = bilateral; L = left; R = right; MNI = Montreal Neurological Institute.

Table 3

Significant positive and negative psychophysiological interaction (PPI) with the dorsal anterior cingulate cortex (dACC) during response preparation

Peak	Side	BA	MNI coordinates			Cluster size (κ)	*T*-value
			x	*y*	*z*		
Positive							
Perigenual anterior cingulate cortex	R	32	18	42	0	159	7.42
Anterior rostral cingulate zone (dACC)	B	32	16	34	18	358	9.47
Posterior rostral cingulate zone (dACC)	R	32	14	14	44	773	9.70
Posterior rostral cingulate zone (dACC)	L	32	−14	2	34	625	8.42
Caudal cingulate zone (dACC)	R	32	18	−28	46	251	7.24
Dorsolateral prefrontal cortex	L	46	−32	34	18	301	6.46
Frontal operculum	R	44	60	10	24	126	5.96
Middle temporal gyrus	R	21	42	−54	0	1,269	6.70
Cerebellum	L	---	−18	−62	−30	475	6.15
Caudate nucleus	B	---	12	2	16	721	4.08
Negative							
Posterior cingulate cortex	R	23	4	−50	16	369	4.61
Pre-supplementary motor area	L	6	0	16	66	175	4.01
Ventral premotor cortex	L	6	−42	4	56	111	5.06
Lingual gyrus	R	18	12	−84	−18	890	5.00
Thalamus	L	---	−2	−8	8	169	3.90

Note: BA = Brodmann area; B = bilateral; L = left; R = right; MNI = Montreal Neurological Institute.

Table 4

BOLD signal increases for response preparation elicited by left and right ready cues

Peak	Side	BA	MNI coordinates			Cluster size (κ)	*T*-value
			x	*y*	*z*		
Left ready cues							
Dorsal anterior cingulate cortex (dACC)	R	32	10	12	38	523	4.32
Inferior frontal gyrus	R	9 / 44	44	12	30	954	5.21
Premotor cortex	L	6	−36	−2	36	1,014	5.99
Superior parietal lobule	R	7	34	−68	30	1,056	7.81
Fusiform gyrus	R	19	40	−64	−14	1,155	8.00
Fusiform gyrus	L	18	−24	−86	4	2,585	6.95
Right ready cues							
Dorsal anterior cingulate cortex (dACC)	L	32	−8	12	38	114	4.24
Premotor cortex / inferior frontal gyrus	R	6 / 44	32	−2	52	886	4.75
Premotor cortex	L	6	−36	−6	52	652	3.70
Fusiform gyrus	R	37	−46	−62	−10	4,338	7.12
Fusiform gyrus	L	37	−36	−58	−10	4,260	6.80

Note: BA = Brodmann area; L = left; R = right; MNI = Montreal Neurological Institute.

Table 5

Significant psychophysiological interaction (PPI) with the right and left dorsal anterior cingulate cortex (dACC) for response preparation elicited by left and right ready cues respectively

Peak	Side	BA	MNI coordinates			Cluster size (κ)	*T*-value
			x	*y*	*z*		
Left ready cues (right dACC)							
Dorsolateral prefrontal cortex (DLPFC)	L	46	−36	40	14	472	7.26
Premotor cortex	R	6	36	−4	52	535	6.14
Supplementary motor area	R	6	10	6	50	1,774	7.93
Anterior insula	R	---	36	16	2	927	4.86
Posterior insula	L	---	−44	−6	4	647	5.53
Inferior parietal lobule	R	40	52	−32	50	2,472	6.14
Inferior parietal lobule	L	40	−64	−30	36	1,240	4.86
Middle temporal gyrus	R	21	46	−52	2	123	4.22
Caudate nucleus	L	---	−8	16	4	101	4.30
Right ready cues (left dACC)							
Ventrolateral prefrontal cortex	L	10	−40	52	12	677	4.53
Frontal operculum / DLPFC	R	44	40	6	38	3,340	6.35
Supplementary motor area	L	6	−8	10	48	4,356	8.81
Anterior insula	L	---	−42	2	4	424	5.88
Middle occipital gyrus	R	19	34	−78	24	6,432	5.40
Inferior temporal gyrus	R	37	50	−46	−14	638	5.04
Inferior temporal gyrus	L	37	−42	−62	−12	625	4.71
Cerebellum	R	---	4	−72	−22	312	5.25
Cerebellum	L	---	−42	−58	−32	206	3.73

Note: BA = Brodmann area; L = left; R = right; MNI = Montreal Neurological Institute.

Table 6

BOLD signal increases for general response effects and specific to response inhibition

Peak	Side	BA	MNI coordinates			Cluster size (κ)	*T*-value
			x	*y*	*z*		
General response effects							
Frontal operculum	L	44	−56	6	26	1,238	10.12
Supplementary motor area	B	6	6	−2	66	2,195	10.31
Anterior insula cortex	R	---	34	18	6	1,749	8.56
Primary motor cortex	R	4	30	−26	62	103	4.79
Primary motor cortex	L	4	−36	−10	62	121	4.96
Inferior parietal lobule	R	40	40	−46	54	2,558	7.85
Inferior parietal lobule	L	40	−44	−34	48	2,326	11.87
Cerebellum	B	---	36	−42	−26	5,091	10.15
Thalamus	L	---	−12	−14	6	652	7.53
Response inhibition							
Inferior frontal gyrus (pars orbitalis)	L	47	−34	34	−16	219	8.10
Inferior frontal gyrus (pars triangularis)	R	45	48	22	8	249	7.32
Middle frontal gyrus	R	8	32	24	56	2,176	8.98
Ventral premotor cortex	L	6	−38	10	56	4,040	9.39
Temporoparietal cortical junction	R	40	52	−54	28	1,235	8.86
Temporoparietal cortical junction	L	22	−64	−42	2	2,098	7.82
Middle temporal gyrus	R	21	54	2	−20	645	10.51
Middle occipital gyrus	R	19	42	−76	−6	508	7.00

Note: BA = Brodmann area; B = bilateral; L = left; R = right; MNI = Montreal Neurological Institute.